Resolving the Two Monolayers of a Lipid Bilayer in Giant Unilamellar Vesicles Using Deuterium Nuclear Magnetic Resonance†

Francesca M. Marassi,‡ Richard R. Shivers,§ and Peter M. Macdonald*,‡

Department of Chemistry and Erindale College, University of Toronto, Toronto, Ontario, Canada, and Department of Zoology, University of Western Ontario, London, Ontario, Canada

Received May 6, 1993; Revised Manuscript Received July 12, 1993®

ABSTRACT: Giant unilamellar vesicles (GUVs) composed of mixtures of POPC (1-palmitoyl-2-oleoyl-*sn*-glycero-3-phosphocholine) plus DMPG (1,2-dimyristoyl-*sn*-glycero-3-phosphoglycerol) and/or CHOL (cholesterol) were prepared using detergent dialysis. Vesicles containing at least 30 mol % CHOL had diameters exceeding 450 nm. POPC in such GUVs, deuterium-labeled at either the choline α or β segments, yielded deuterium (^{2}H) and phosphorus (^{31}P) nuclear magnetic resonance (NMR) Pake pattern line shapes, quadrupole splittings and chemical shift anisotropies identical to those obtained with multilamellar vesicles (MLVs) of identical composition. Exposing exclusively the vesicle exterior to either calcium or perchlorate ions, both of which are known to influence lipid head-group conformation through surface charge effects, caused the appearance of two overlapping ^{2}H Pake patterns of equal intensity. The quadrupole splitting of one component remained unchanged while that of the second component was altered in the manner expected for choline α or β deuterons in the presence of a cationic (calcium) or anionic (perchlorate) surface charge. Freeze–thawing the GUVs to equilibrate the exterior and interior vesicular contents eliminated the initially unchanged spectral component. It was likewise possible to resolve two quadrupole splittings when *Staphylococcus aureus* δ-toxin, a surface-active peptide known to influence lipid head-group orientational ordering, was added to the exterior vesicular solution only. This indicates that δ-toxin upon binding remains confined to one monolayer of the lipid bilayer and does not traverse the membrane. We conclude that ^{2}H NMR can resolve differences in lipid conformation and orientational order at the two monolayers of a lipid bilayer in GUVs and should prove useful in probing transbilayer asymmetries of lipid composition, protein orientation, ion distribution, and ligand binding.

Solid-state deuterium (^{2}H) and phosphorus (^{31}P) nuclear magnetic resonance (NMR)[1] techniques have provided a wealth of information concerning structure and dynamics in lipid bilayer membranes [for reviews see Seelig (1977), Griffin (1981), and Davis (1983)]. With few exceptions (Ryba et al., 1986; Bayerl & Bloom, 1990; Gale & Watts, 1992), such investigations have employed multilamellar vesicles (MLVs). Because MLVs spontaneously form large diameter, essentially planar lipid bilayers upon dispersion in water, they are an attractive and convenient system in which to model processes occurring in real biological membranes. However, there are a multitude of important membrane-associated biological phenomena which are impossible to model in MLVs because of their onionskin-like architecture. Specifically, in MLVs one cannot impose a transmembrane electrical potential, nor induce a transbilayer asymmetry of lipid distribution or protein orientation, nor probe asymmetric interactions with interior versus exterior vesicular solution. In short, using MLVs one cannot resolve differences between the inner and the outer monolayer of a lipid bilayer.

All of these features of biological membranes can be modeled in unilamellar lipid vesicles. In such vesicles the lipids are distributed between two and only two populations, those facing the interior and those facing the exterior of the vesicle. In principle, it should be possible to employ ^{2}H and ^{31}P NMR to resolve any differences in conformation and orientational ordering between the two lipid populations arising due to the transmembrane asymmetries mentioned above. In practice, not all unilamellar vesicles are appropriate for the purposes of solid-state ^{2}H and ^{31}P NMR, since for small vesicles overall vesicle tumbling and lipid lateral diffusion can adversely affect the NMR spectral line shape. Theoretical predictions (Stockton et al., 1976; Burnell et al., 1980) indicate that the critical vesicle diameter is in the region of 500 nm. Unilamellar vesicles prepared by sonication (diameter 20–50 nm, Saunders et al., 1962) or by size extrusion (diameter 50–300 nm, Hope et al., 1985), for example, are simply too small to provide solid state ^{2}H and ^{31}P NMR spectra free from complications arising due to vesicle size effects. Unilamellar vesicles with diameters exceeding 400 nm have been prepared using a detergent dialysis method (Goldin, 1977).

In this report we describe several novel applications of ^{2}H and ^{31}P NMR in giant unilamellar vesicles (GUVs) prepared by the method of detergent dialysis. We confirm experimentally the theoretical prediction that the critical vesicle size is in the region of 500 nm. We show that the ^{2}H and ^{31}P NMR line shapes in GUVs permit the same depth of analysis of conformation and orientational ordering as provided by MLVs. Furthermore, we demonstrate for the first time that

† This work was supported by the National Science and Engineering Research Council of Canada.

* Author to whom correspondence should be addressed.
‡ University of Toronto.
§ University of Western Ontario.

® Abstract published in *Advance ACS Abstracts,* September 1, 1993.

[1] Abbreviations: NMR, nuclear magnetic resonance; QELS, quasi-elastic light scattering; FFEM, freeze–fracture electron microscopy; GUV, giant unilamellar vesicles; MLV, multilamellar vesicles; $\Delta\nu$, quadrupole splitting; $\Delta\sigma$, chemical shift anisotropy; T_1, spin–lattice relaxation time; T_2, spin–spin relaxation time; POPC, 1-palmitoyl-2-oleoyl-*sn*-glycero-3-phosphocholine; POPA, 1-palmitoyl-2-oleoyl-*sn*-glycero-3-phosphate; DMPG, 1,2-dimyristoyl-*sn*-glycero-3-phosphoglycerol; CHOL, cholesterol; OG, *n*-octyl β-glucopyranoside; HEPES, 4-(2-hydroxyethyl)piperazine-1-ethanesulfonic acid; TPS, 2,3,5-triisopropylbenzenesulfonyl chloride.

0006-2960/93/0432-9936$04.00/0

in GUVs one may resolve differences in lipid conformation and orientational ordering at the two monolayers of a unilamellar vesicle's bilayer. Finally, we illustrate how this new capability can provide definitive answers regarding the configuration of membrane-associating peptides.

MATERIALS AND METHODS

Materials. Nondeuterated lipids were purchased from Avanti Polar Lipids (Alabaster, AL). *n*-Octyl β-glucopyranoside (OG) was purchased from Sigma (St. Louis, MO). 4-(2-Hydroxyethyl)piperazine-1-ethanesulfonic acid (HEPES) was purchased from BDH (Toronto, ON). 2,3,4-Triisopropylbenzenesulfonyl chloride (TPS) was purchased from Aldrich (Milwaukee, WI) and was recrystallized from *n*-pentane prior to use. Cholesterol (CHOL) was purchased from Fisher (Ottawa, ON) and was recrystallized from ethanol prior to use.

Synthesis of Head Group Deuterated Lipids. The structure of the phosphocholine head group is shown below. The α and β nomenclature employed for the deuterium-labeled segments is also indicated. 1-Palmitoyl-2-oleoyl-*sn*-glycero-3-phosphocholine (POPC) was selectively deuterated at the choline α or β segments by a combination of the methods of Harbisson and Griffin (1984) and Aloy and Rabaut (1913). POPC-α-d_2 and POPC-β-d_2 were prepared by coupling 1-palmitoyl-2-oleoyl-*sn*-glycero-3-phosphate (POPA) with choline tetraphenylboron salt, selectively deuterated at the α or β segments, using TPS as the condensing agent (Aneja et al., 1970). The deuterated phosphatidylcholines were purified by chromatography on silica gel, followed by chromatography on CM-52 as described by Comfurius and Zwaal (1977), and their purity was checked by thin-layer chromatography and ^{1}H NMR.

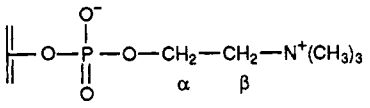

MLV Preparation. Typically, 20 mg of deuterated POPC plus the desired amounts of other lipids, all in chloroform/methanol (2/1 v/v), were mixed by vortexing, and the solvents were removed under a stream of nitrogen, followed by several hours under high vacuum. The dried lipids were dispersed in excess NaCl buffer (150 mM NaCl and 10 mM HEPES, pH 7.0) by vortexing and warming to 40 °C.

GUV Preparation. OG was added to the MLV dispersion described above in an overall detergent-to-lipid molar ratio of 12/1, yielding a clear micellar solution. The detergent–lipid mixture was injected into the dialysis cell of a Minilipoprep dialyzer (Avestin, Ottawa, ON) and dialysed through a cellulose membrane (molecular weight cutoff 10 000, Diachema, Switzerland) against 1000 mL of NaCl buffer. Dialysis continued for 48 h with four changes of the buffer medium. Vesicle formation resulted in a cloudy suspension which could be used directly for NMR measurements.

Exchange of the External Vesicle Solution. About 1 ml of GUV suspension was first concentrated to a minimal volume by centrifugation through a Centriprep-10 microconcentrator (Amicon, Canada) for 30 min at 4500*g*. The GUV suspension was reconstituted to its original volume with the desired buffering solution (150 mM $NaClO_4$ and 10 mM HEPES, pH 7.0, or 100 mM $CaCl_2$ and 10 mM HEPES, pH 7.0). Effectively total exchange of the external vesicle solution was judged to have been achieved after four such concentration–reconstitution cycles.

Table I: Vesicle Diameters and Polydispersities Measured by Quasi-Elastic Light Scattering[a]

vesicle composition (molar ratio)	vesicle diameter, d (nm)	size polydispersity, P
POPC (100%)	186	0.04
POPC/CHOL (90/10)	318	0.03
POPC/CHOL (70/30)	450	0.12
POPC/DMPG/CHOL (60/10/30)	815	0.06
POPC/DMPG/CHOL (50/20/30)	837	0.02
POPC/DMPG/CHOL (40/30/30)	836	0.05

[a] The polydispersity is defined as $P = \sigma^2/d^2$, where σ is the standard deviation.

δ-Toxin Addition. δ-Toxin from *Staphylococcus aureus* (strain NCTC 10345) was isolated and characterized as described previously (Rydall & Macdonald, 1992b). δ-Toxin was dissolved in the same NaCl buffer used to hydrate the lipids. An aliquot containing the desired amount of peptide was added directly to the GUVs in the NMR tube to give a final lipid-to-peptide ratio of 25/1.

NMR Measurements. ^{2}H NMR spectra were recorded on a Chemagnetics CMX300 NMR spectrometer operating at 45.98 MHz, using a Doty broad-line probe equipped with a 10-mm-diameter solenoid coil and high-power proton decoupling. The quadrupole echo pulse sequence (Davis et al., 1976) was employed using quadrature detection with complete phase cycling of the pulse pairs and a 90° pulse length of 6.5 μs, an interpulse delay of 40 μs, a recycle delay of 100 ms, a spectral width of 100 kHz, and a 2K data size. The longitudinal relaxation time (T_1) was measured using the combined inversion recovery–quadrupole echo pulse sequence (180_x–τ–90_x–t–90_y–t–ACQ).

^{31}P NMR spectra were recorded with the same Doty probe at 121.25 MHz using a Hahn echo sequence (Rance & Byrd, 1983) with proton decoupling and a 90° pulse width of 10.5 μs, an echo spacing of 40 μs, a recycle delay of 2 s, a spectral width of 100 kHz, and a data size of 2K.

Quasi-Elastic Light Scattering. Quasi-elastic light scattering (QELS) measurements were performed on a BI-90 particle sizer from Brookhaven Instruments using a He–Ne laser at a fixed scattering angle of 90°, at a temperature of 23 °C. For each vesicle lipid composition three samples were prepared, each of which was measured 10 times to yield the average diameters reported in Table I. For a detailed discussion of QELS the reader is referred to the monograph by Berne and Pecora (1976). The measurement provides the mean diameter, d, and the polydispersity, P, of particle sizes, which is related to the standard deviation, σ, of the size distribution through the equality $P = \sigma^2/d^2$.

Freeze–Fracture Electron Microscopy. Vesicles were prepared for freeze–fracture electron microscopy (FFEM) by suspension of the particles (ca. 40% by weight) in distilled water. Single droplets of this suspension were placed on gold specimen discs (Balzers, Liechtenstein) and frozen in a slurry of liquid nitrogen-cooled freon-22. Each droplet was approximately 1.4–1.8 mm in diameter. Frozen discs were stored in liquid nitrogen until further processing was undertaken.

Freeze–fracture of the frozen particle suspensions was carried out at −115 °C in a Balzers BAF 301 freeze-etch unit (Balzers, Liechtenstein) in a vacuum of 10^{-6} Torr, following the general procedure of Shivers and Brightman (1976). The exposed surface of the vesicle suspension was replicated with a thin film (ca. 60 nm) of platinum and carbon. The platinum

was evaporated onto the fracture surface at an angle of 45°, and carbon was evaporated onto the surface at 90°. All platinum replicas were cleaned in filtered sodium hypochlorite (Javex) for at least 2 h at room temperature. Replicas that were left in bleach overnight were the cleanest. Cleaned replicas were rinsed in three changes of filtered distilled water and then picked up on bare 200-mesh copper grids. The replicas were examined in a Philips 201 electron microscope operating at 60 kV. Vesicles were initially photographed at 30 000 diameters and then were further enlarged photographically.

RESULTS AND DISCUSSION

GUVs Yield ^2H and ^{31}P NMR Spectra Uncomplicated by Vesicle Size Effects. The diameters and polydispersities of the various vesicle preparations as measured using QELS are reported in Table I. The vesicle size varies systematically with lipid composition. Increasing the amount of cholesterol up to 30 mol % leads to a greater than 2-fold increase in vesicle diameter, relative to pure POPC vesicles. This influence of cholesterol on vesicle size has been noted previously (Gent & Prestegard, 1974; Rhoden & Goldin, 1979; Philippot et al., 1983). The further addition of just 10 mol % DMPG leads to an additional 2-fold increase in vesicle diameter.

The polydispersity parameter provides an estimate of the width of the vesicle size distribution. Values of P between 0.02 and 0.08 are typical of narrow size distributions. The data in Table I indicate that, for most of the lipid compositions investigated here, narrow vesicle size distributions are obtained. For the composition 70/30 POPC/CHOL (all proportions are molar ratios), exponential sampling analysis of the light-scattering data (Pike, 1981) indicates a bimodal distribution of vesicle sizes with peaks at vesicle diameters of 450 and 2000 nm. The peak at 450 nm is 99% by intensity as well as by number, while the peak at 2000 nm is 1% by intensity as well as by number.

Freeze–fracture electron microscopy (FFEM) on vesicles composed of either 70/30 POPC/CHOL or 50/30/20 POPC/CHOL/DMPG shows unilamellar vesicles, with diameters comparing favorably with those obtained by QELS. For the 50/30/20 POPC/CHOL/DMPG vesicles, FFEM indicates a uniform size distribution. For the 70/30 POPC/CHOL vesicles FFEM indicates a bimodal distribution of vesicle sizes in which a small population of large vesicles appears to arise as a result of aggregation of smaller vesicles.

We refer to the vesicles prepared by detergent dialysis and containing DMPG and/or 30% CHOL as giant unilamellar vesicles (GUV) in order to emphasize their greater size relative to the large unilamellar vesicles (LUV) synthesized by extrusion techniques. The vesicle size and size distribution effects of CHOL and DMPG may be understood in light of the membrane micromechanical studies of Evans and Needham (1987), who noted that vesicle rupture occurs when dilation of the bilayer surface area causes critical fluctuations in the lipid surface density. Bilayers with lower lipid area compressibility can withstand higher tension levels for rupture and, hence, exhibit enhanced cohesion. The addition of CHOL to phospholipid membranes greatly reduces bilayer compressibility and enhances bilayer cohesion. Therefore, it is likely that CHOL allows larger vesicles to grow by providing mechanical strength to the bilayer membrane. The equally dramatic effect of DMPG on vesicle size may be related either to a reduced bilayer compressibility in the presence of an anionic lipid (Evans & Needham, 1987) or to the details of the dialysis procedure. The formation of GUVs by detergent

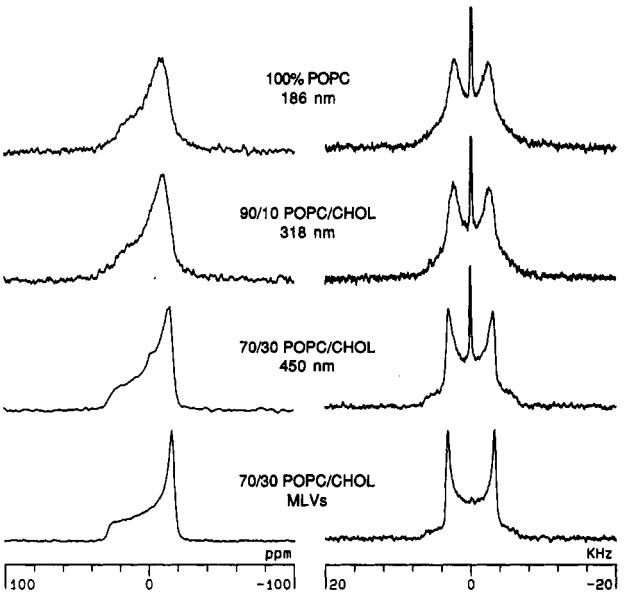

FIGURE 1: Effect of vesicle size on phospholipid ^{31}P and ^2H NMR spectral line shapes. ^{31}P (left) and ^2H (right) NMR spectra from POPC-α-d_2 were recorded at 23 °C from unilamellar vesicles of compositions (proceeding from the top) 100% POPC, 90/10 POPC/CHOL, and 70/30 POPC/CHOL. The bottom spectra were recorded with multilamellar vesicles of composition 70/30 POPC/CHOL. The vesicle diameters as measured using QELS (see Table I) are indicated.

dialysis requires effective dispersion of the lipids by the detergent. Removal of the detergent increases the number of contacts between the lipid hydrocarbon chains until a critical concentration marks the onset of vesiculation (Lasic, 1982). Dialysis affords a slow and controlled rate of detergent removal and, hence, of lipid aggregation, allowing larger unilamellar vesicles to form. Intervesicular electrostatic repulsions due to anionic DMPG should aid lipid dispersion considerably and promote the formation of larger vesicles.

Figure 1 illustrates the corresponding ^{31}P NMR (left) and ^2H NMR (right) spectra for unilamellar vesicles of various sizes containing choline-deuterated POPC. ^2H NMR line shapes are sensitive to the details of vesicle tumbling and lipid lateral diffusion rates in the regime where $\omega_q^2 \tau_v^2 \leq 1$, where ω_q is the static quadrupole coupling constant ($2\pi \times 170$ kHz for aliphatic deuterons) and τ_v is the lipid effective motional correlation time, for which according to the above inequality a critical value occurs in the region $\tau_v \approx 4 \times 10^{-5}$ s. Following Bloom et al. (1975), for a lipid in a spherical vesicle of radius r, undergoing isotropic rotational motion, τ_v has two contributions: τ_r, the correlation time for vesicle tumbling, and τ_d, the correlation time for translational diffusion of the lipid around the bilayer surface, as described by

$$\frac{1}{\tau_v} = \frac{1}{\tau_r} + \frac{1}{\tau_d} = \frac{3kT}{4\pi\eta r^3} + \frac{6D_d}{r^2} \quad (1)$$

From the vesicle radius one estimates τ_r by means of the Stokes–Einstein relation where k is the Boltzmann constant, T is the temperature in Kelvin, and η is the viscosity of the suspending liquid (0.8904 cP for water). τ_d is estimated from the vesicle radius and the translational diffusion coefficient, D_d, which for phosphatidylcholine is around 10^{-8} cm^2/s (Edidin, 1981).

The ^{31}P NMR spectra from vesicles composed of 100% POPC and 90/10 POPC/CHOL show some effects of isotropic motional narrowing, evident as a rounding of the features of the spectral line shape relative to the MLV spectrum.

Furthermore, their chemical shift anisotropies ($\Delta\sigma$), measured as the frequency separation between the low-field and the high-field shoulders, are reduced relative to the values measured in MLVs. These vesicles have diameters of 186 and 318 nm, respectively, leading to corresponding effective motional correlation times, τ_v, of 4.8×10^{-4} and 2.0×10^{-3} s (calculated assuming $D_d = 10^{-8}$ cm^2/s), respectively. Since these correlation times are longer than the critical correlation time estimated above, one expects the spectral line shapes to be predominantly anisotropic, as indeed they are. Increasing the vesicle diameter to 450 nm ($\tau_v = 4.6 \times 10^{-3}$ s) through addition of 30 mol % cholesterol yields a spectrum closely similar to that obtained with MLVs and having $\Delta\sigma$ equal to −47 ppm, identical to the value measured in MLVs.

Similar vesicle size effects are observable in the ^{2}H NMR spectra. Vesicles with diameters of 186 and 318 nm show spectra with a noticeable degree of isotropic motional narrowing. The respective quadrupole splittings ($\Delta\nu$), measured as the frequency separation between the maxima of each spectrum, are reduced in size relative to the values measured in MLVs of identical composition. On the other hand, vesicles 450 nm in diameter yield a spectrum with a line shape similar to that observed for MLVs and having a quadrupole splitting of 6.26 kHz, identical to the value measured from MLVs.

The results displayed in Figure 1 indicate that, to obtain reliable measurement of ^{31}P NMR chemical shift anisotropies and ^{2}H NMR quadrupole splittings free from complications due to vesicle tumbling, one must employ vesicles with diameters on the order 450 nm or greater. This result confirms the theoretical predictions of Burnell et al. (1980) and Stockton et al. (1976), who reached similar conclusions by means of ^{31}P and ^{2}H NMR line shape simulations. Note that even for the 450-nm-diameter vesicles the NMR line shapes appear slightly rounded. This may be due to a distribution of vesicle sizes centred around the critical diameter of 450 nm or to local thermal undulations of the lipid bilayers affecting the local order parameter.

The fact that both the chemical shift anisotropy and the quadrupole splitting are identical in MLVs and in GUVs 450 nm in diameter indicates that both the orientational order and the average conformation of the choline head group of POPC are probably the same in the two model membrane systems. Note, however, that a set of quadrupole splittings for the choline head group does not uniquely specify a single head group conformation (Skarjune & Oldfield, 1979). Our ^{2}H NMR spin–lattice (T_1) relaxation time measurements yield similar values in GUVs (17.3 ms) and MLVs (15.3 ms) composed of 70/30 POPC/CHOL, implying that the head group intramolecular motions have similar correlation times in the two systems.

Note that the central isotropic peak in the GUV spectra is attributable to the natural-abundance ^{2}H in water, since it is impractical to employ deuterium-depleted water in the preparation of GUVs and since their water content far exceeds that of a comparable MLV preparation. No such isotropic component is observed by ^{31}P NMR, confirming the absence of any isotropic lipid phase. The intensity of the central isotropic peak in the GUV ^{2}H NMR spectrum can lead to dynamic range problems if not somehow suppressed. Fortunately, the T_1 of water is on the order of seconds, while the T_1 of the choline deuterons is on the order of milliseconds. The ^{2}H NMR spectra in Figure 1 were obtained using a recycle delay of 100 ms, so that the intensity of the central water resonance line is largely suppressed without adversely affecting the signal intensity from the lipid head group deuterons.

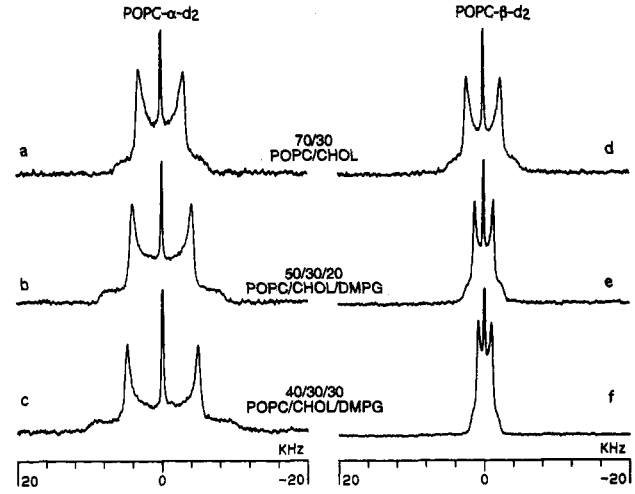

FIGURE 2: Effect of increasing surface charge on the ^{2}H NMR spectrum in GUVs. ^{2}H NMR spectra from POPC-α-d_2 (left) and POPC-β-d_2 (right) were recorded at 23 °C from GUVs of compositions (proceeding from the top) 70/30 POPC/CHOL, 50/30/20 POPC/CHOL/DMPG, and 40/30/30 POPC/CHOL/DMPG, as indicated in the figure.

The presence of cholesterol in these vesicles leads to increased vesicle size but has little apparent influence on the internal lipid head group conformation or dynamics discernible by ^{2}H or ^{31}P NMR. This is not unexpected since chemical shift anisotropies and quadrupole splittings measured in MLVs containing POPC with or without cholesterol are identical (Brown and Seelig, 1978). Likewise, Browning (1981) reported virtually identical values for the T_1 of the choline head group in MLVs containing DPPC with or without cholesterol.

Conformation Changes of the Phosphatidylcholine Head Group Can Be Determined in GUV Using ^{2}H NMR. The head group of phosphatidylcholine undergoes a pronounced conformation change in response to the presence of surface charge which is readily detected in MLVs using ^{2}H NMR (Seelig et al, 1987). The ^{2}H NMR spectra in Figure 2 demonstrate that the same conformation change occurs in GUVs and is detectable via ^{2}H NMR. The bilayer surface charge was made progressively more anionic by increasing the proportion of DMPG in the GUV lipid mixture at the expense of POPC while maintaining the CHOL content at a constant 30%. The ^{2}H NMR spectra from such GUVs containing POPC-α-d_2, on the left in the figure, reveal that the quadrupole splitting increases with increasing DMPG content from the top spectrum to the bottom. Conversely, the quadrupole splitting decreases with increasing DMPG content when the ^{2}H NMR spectra from GUVs containing POPC-β-d_2 are recorded, as shown on the right in the figure. Such a counterdirectional change in the size of the quadrupole splitting from POPC-α-d_2 versus POPC-β-d_2 is characteristic of the unique, concerted conformation change undergone by the phosphatidylcholine head group in response to a surface charge potential, in this case negative surface charge. Quantitatively, the values of the quadrupole splittings correspond precisely with those measured for identical proportions of DMPG in mixed DMPG/DMPC MLVs (Macdonald et al., 1991).

It is interesting that the presence of 30% CHOL has no apparent effect on the sensitivity of the phosphatidylcholine head group to surface charges. CHOL, being neutral, should not itself contribute to the bilayer surface charge density other than through a dilution effect. To the best of our knowledge

this is the first evidence pertaining specifically to the effect of CHOL on the surface charge response of phosphatidylcholine.

Since each of the spectra in Figure 2 consists of a single Pake pattern characterized by a single quadrupole splitting, it follows that all the lipid molecules in the entire vesicle (indeed the entire sample) experience an identical environment. This is consistent with the supposition that POPC, DMPG, and CHOL form homogeneous mixtures in the ratios employed here, while there is no reason to expect any transbilayer asymmetry of lipid distribution.

Finally, the fact that GUVs and MLVs containing identical proportions of DMPG yield identical quadrupole splittings indicates that the conformation change undergone by the choline head group is not influenced by interlamellar electrostatic interactions, such as those present in MLVs but largely absent in GUVs. This was a point of some controversy in earlier ^{2}H NMR investigations of membrane surface charge effects.

^{2}H NMR Can Resolve Differences in Surface Charge at the Two Monolayers of a GUV Lipid Bilayer. The surface charge density at the internal and external surfaces of a biomembrane can differ for a number of reasons, including asymmetries of transbilayer lipid distribution or protein composition, transmembrane gradients of ion concentration or pH, and preferential ligand (peptides, drugs, anesthetics) binding to an exposed versus a cryptic surface. Our goal is to determine whether such an asymmetric charge distribution is detectable using ^{2}H NMR.

A simple means of generating a transbilayer surface charge asymmetry is to expose the exterior of GUVs to $NaClO_4$. ^{2}H NMR studies in MLVs indicate that perchlorate ions, but not sodium ions, bind with high affinity to POPC membrane surfaces and in so doing generate a large negative surface charge density (Macdonald & Seelig, 1988; Rydall & Macdonald, 1992a). Since perchlorate is an aqueous ion, it will not permeate the vesicle membrane and the interior vesicle solution will remain perchlorate-free.

Figure 3 illustrates the effects on the ^{2}H NMR spectra from 70/30 POPC/CHOL GUVs containing POPC-α-d_2 (left) or POPC-β-d_2 (right) when the external vesicle solution is exchanged for a buffer containing 150 mM $NaClO_4$. In the absence of perchlorate the ^{2}H NMR spectra consist of single Pake patterns as discussed above (spectra a and e). Addition of 150 mM perchlorate ions to the external vesicle solution leads to the appearance of a second overlapping Pake pattern in both the POPC-α-d_2 and POPC-β-d_2 spectra (spectra b and f). The quadrupole splitting from one Pake component remains unchanged from that measured in the absence of perchlorate (6.26 and 4.59 kHz for POPC-α-d_2 and POPC-β-d_2, respectively), indicating that it arises from a population of lipids sequestered from exposure to perchlorate ions. The quadrupole splitting from the second Pake component changes in a manner indicative of the presence of negative surface charges (increasing to 8.68 kHz for POPC-α-d_2 and decreasing to 2.17 kHz for POPC-β-d_2). It follows that this second population of lipids must be exposed to perchlorate binding. The presence of two overlapping Pake patterns in the ^{2}H NMR spectra, and hence the distinction between the two lipid populations—one exposed to and one sequestered from perchlorate—persists in such samples for at least 12 h.

The prolonged existence of these two distinct lipid populations depends on the integrity of the lipid bilayer as a permeability barrier. When perchlorate ions are added to the external GUV solution and the vesicles are subjected to a

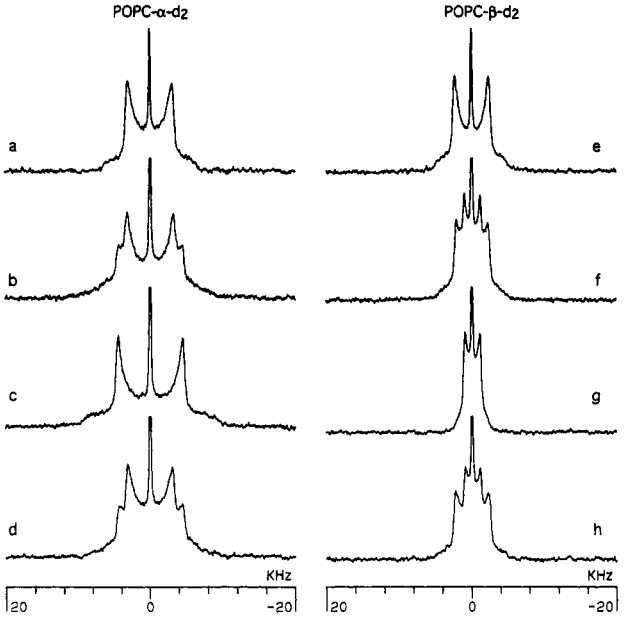

FIGURE 3: Effect of an asymmetric perchlorate ion distribution on the ^{2}H NMR spectra measured at 23 °C from GUVs containing 70/30 POPC/CHOL. Spectra on the left side are from POPC-α-d_2. Spectra on the right side are from POPC-β-d_2. (a and e) Initial spectra prior to ClO_4^- addition. (b and f) 150 mM ClO_4^- added to vesicle exterior. (c and g) End point spectra after freeze–thawing. (d and h) Addition spectra generated from the 1:1 addition of the initial and end point spectra (a + c and e + g).

cycles of freeze–thawing, which rupture the bilayer and allows the external and internal vesicle solutions to equilibrate, the resulting ^{2}H NMR spectra again consist of single Pake patterns (spectra c and g). The size of the single quadrupole splittings (8.68 kHz for POPC-α-d_2 and 2.17 kHz for POPC-β-d_2) indicates that this single population of lipids is entirely exposed to perchlorate ion binding.

Do these two populations of lipids correspond to the inner and outer monolayer of the GUV lipid bilayer? Or is it possible that some portion of the vesicles in the sample are actually multilamellar in architecture, leading, thereby, to similar "two-population" spectra which reduce to a "one-population" spectra following freeze–thaw cycling? We can distinguish these two possibilities on the basis of the relative contributions of the two Pake patterns in the "two-population" spectra of Figure 3. If the entire sample of vesicles is unilamellar, then the ratio of the lipid populations represented by the two Pake patterns should be 1:1. If a portion of the vesicles are multilamellar, then the ratio of the lipid populations represented by the two Pake patterns should deviate proportionately from 1:1. In Figure 3 the bottom spectra (d and h) were obtained by adding together in a 1:1 ratio the perchlorate-free and fully perchlorate-exposed spectra (a + c and e + g). It is evident that this simple 1:1 addition of the end-point "one-population" spectra reproduces in every essential detail the "two-population" spectra. We conclude that these two lipid populations indeed correspond to the inner and outer monolayers of the lipid bilayer of unilamellar vesicles. Note that a spectral simulation of the "two-population" spectra could provide the ratio of the signal intensities contributed by the two Pake pattern components. However, NMR signal intensities are influenced not only by the number of spins but also by the relaxation times T_1 and T_2. The latter might differ in the presence versus the absence of perchlorate (or any other ligand). The end-point spectral addition procedure avoids any possible ambiguity since all relaxation time effects are automatically taken into account.

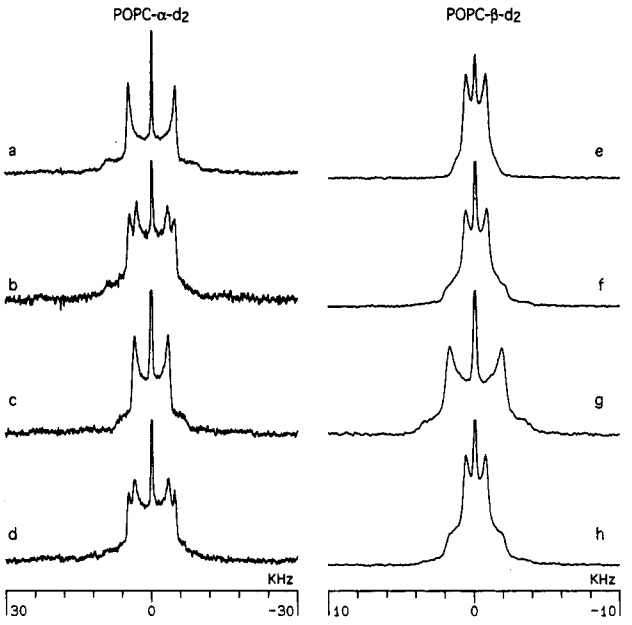

FIGURE 4: Effect of an asymmetric calcium ion distribution on the ^{2}H NMR spectra measured at 23 °C from GUVs containing 40/30/30 POPC/CHOL/DMPG. Spectra on the left side are from POPC-α-d_2. Spectra on the right side are from POPC-β-d_2. (a and e) Initial spectra prior to Ca^{2+} addition. (b and f) 100 mM Ca^{2+} added to vesicle exterior. (c and g) End point spectra after freeze–thawing. (d and h) Addition spectra generated from the 1:1 addition of the initial and end point spectra (a + c and e + g).

Figure 4 shows the ^{2}H NMR spectra from a similar series of experiments in which $CaCl_2$ was added to GUVs consisting of 40/30/30 POPC/CHOL/DMPG. Calcium is known to bind to the surface of POPC bilayers where it generates a positive surface charge density which is readily detected via ^{2}H NMR of choline-deuterated phosphatidylcholine (Akutsu & Seelig, 1981; Altenbach & Seelig, 1984; Macdonald & Seelig, 1987a,b). These experiments differ from those performed above with perchlorate ions by virtue of the fact that now a cationic ligand is being employed but also because the resulting surface charge will be due to a ternary mixture of cationic (calcium) plus anionic (DMPG) plus zwitterionic (POPC) species.

In the absence of calcium the ^{2}H NMR spectra for both POPC-α-d_2 (left) and POPC-β-d_2 (right) consist of single Pake patterns with quadrupole splittings corresponding to the values expected in the presence of 30% DMPG (spectra a and e). Addition of 100 mM calcium ions to the external vesicle solution leads to the appearance of a second overlapping Pake pattern in the POPC-α-d_2 spectrum (b) and a second, broad component in the POPC-β-d_2 spectrum (f) which is not immediately identifiable as a Pake doublet (but see below). The quadrupole splitting from one Pake component remains unchanged from that measured in the absence of calcium (9.60 and 1.38 kHz for POPC-α-d_2 and POPC-β-d_2, respectively), indicating that it arises from a population of lipids sequestered from exposure to calcium ions. The quadrupole splitting from the second Pake component changes in a manner indicative of a degree of neutralization of the initial negative surface charge density (decreasing to 6.60 kHz for POPC-α-d_2 and increasing to 3.57 kHz for POPC-β-d_2, the latter determined as described below). It follows that this second population of lipids must be exposed to calcium binding. As was observed in the earlier perchlorate experiments, the presence of the two overlapping Pake patterns in the ^{2}H NMR spectra of such samples persists for at least 12 h. Allowing the external and the internal vesicle solutions to equilibrate by subjecting the GUVs to cycles of freeze–thawing results in ^{2}H NMR spectra (c and g) characterized by a single quadrupole splitting (6.60 kHz for POPC-α-d_2 and 3.57 kHz for POPC-β-d_2), the values of which indicate that this single population of lipids is completely exposed to calcium ion binding. So the maintenance of two distinct lipid populations is once again dependent on the integrity of the lipid bilayer as a permeability barrier. In Figure 4 the bottom spectra (d and h) were obtained by adding together in a 1:1 ratio the calcium-free and fully calcium-exposed spectra (a + c and e + g). It is evident that once again a simple 1:1 addition of the end-point "one-population" spectra reproduces the "two-population" spectra. We conclude that the two lipid populations correspond to the inner and outer monolayers of the lipid bilayer of unilamellar vesicles.

There exist some obvious limits to the resolution achievable with this ^{2}H NMR technique. For instance, in the case of asymmetric addition of calcium to GUVs containing POPC-β-d_2 (spectrum f) it is not certain from visual examination that two distinct spectral components are present or that both correspond to Pake patterns. Only when the addition spectrum (h) is found to reproduce so closely the "two-population" spectrum (f) does the degree of certainty increase, allowing an assignment of a value for the quadrupole splitting. The digital resolution in such spectra is 50 Hz/data point and the quadrupole splittings have an uncertainty of only ±100 Hz. However, in addition to the absolute frequency difference, one's ability to resolve any two quadrupole splittings depends on the overall signal to noise, the relative number of deuterons giving rise to the two Pake patterns, and the relaxation times of the deuterons in the different environments. Compare, for example, the "two-population" spectra (b and f) in Figures 3 and 4. In Figure 3, where the two lipid populations differ in their exposure to perchlorate ions, the integrated intensities of the two Pake patterns are approximately equal, indicating little effect of perchlorate ion binding on relaxation and, hence, signal intensity. Consequently, there is little difficulty in resolving the two quadrupole splittings. In Figure 4, where the two lipid populations differ in their exposure to calcium ions, the integrated intensity of the signal from the calcium-exposed lipids appears to be lower than that of the signal from the calcium-free lipids, implying that calcium binding affects the relaxation times of the lipid head groups. Exposure to calcium increases the quadrupole splitting from POPC-β-d_2, and the resulting decrease in signal-to-noise exacerbates any detrimental effects of relaxation times on signal intensity. For POPC-α-d_2, exposure to calcium decreases the quadrupole splitting, which ameliorates any decrease in signal intensity due to relaxation effects, and we can still readily resolve two quadrupole splittings. Another factor of some relevance to the issue of resolution is the greater overall sensitivity of the quadrupole splittings to a given level of cationic versus anionic surface charge, which favors resolution of differences in the former (Beschiaschvili & Seelig, 1991). Similarly, quadrupole splittings from POPC-α-d_2 are often more sensitive to a given level of surface charge than are the values measured from POPC-β-d_2 (Scherer & Seelig, 1989). In instances where resolution enhancement would be desirable, one could resort to de-Paking of the ^{2}H NMR spectra, which doubles the frequency separation between the spectral maxima relative to the usual quadrupole splitting, albeit at the expense of overall signal-to-noise (Sternin et al., 1983).

^{2}H NMR Can Resolve Differences in Orientational Order at the Two Monolayers of a GUV Lipid Bilayer. δ-Toxin is a 26-residue cytolytic, amphipathic peptide, known to lyse a

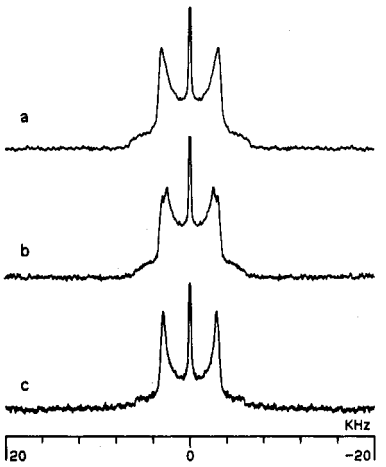

FIGURE 5: Effect of an asymmetric δ-toxin distribution on the ^2H NMR spectra measured at 23 °C from GUVs containing 70/30 POPC-α-d_2/CHOL. (a) Initial spectrum prior to the addition of δ-toxin. (b) After addition of δ-toxin to the vesicle exterior, in a peptide/lipid molar ratio of 1/25.

wide variety of cells and organelles. It binds with high affinity to phospholipid membranes, where it adopts a predominantly α-helical secondary structure (Freer & Arbuthnott, 1982). Two models have been proposed to account for the cytolytic effect of this peptide. In one case, it is proposed that δ-toxin remains localized at the surface of the lipid bilayer but penetrates like a wedge into the bilayer proper to such a degree that it creates defects in the bilayer structure (Terwillinger et al., 1982). In the second case, δ-toxin is proposed to insert into and span the lipid bilayer. Aggregation of the membrane-spanning units could then produce a transmembrane pore which leaks the cell contents (Freer & Birkbeck, 1982).

The ^2H NMR spectra in Figure 5 demonstrate that ^2H NMR in GUVs provides a definitive resolution to the issue of whether δ-toxin adopts a transmembrane or a surface orientation upon binding to lipid bilayer. A recent ^2H NMR investigation from this laboratory showed that in MLVs δ-toxin decreases the quadrupole splitting from both POPC-α-d_2 and POPC-β-d_2, as well as the chemical shift anisotropy of the lipid phosphate group (Rydall & Macdonald, 1992b). These observations indicate that the presence of δ-toxin induces a generalized disordering of the phospholipid head group conformation, as opposed to the type of concerted conformation change apparent in the presence of surface charges. When δ-toxin is added in an overall peptide-to-lipid ratio (mol/mol) of 1/25 to the exterior of GUVs composed of 70/30 POPC/CHOL, the ^2H NMR spectrum from POPC-α-d_2 (spectrum b) consists of a pair of overlapping Pake patterns. The quadrupole splitting of one component remains unchanged relative to the value obtained in the absence of δ-toxin (6.26 kHz), indicating that it arises from a population of lipids sequestered from exposure to the peptide. The quadrupole splitting of the second Pake pattern decreases to a value of 5.00 kHz, which is the behavior expected for a population of lipids exposed to δ-toxin. The presence of two Pake patterns persists in such samples for at least 12 h. We did not perform parallel measurements on GUVs containing POPC-β-d_2 because δ-toxin has only marginal effects on its quadrupole splitting at the levels employed here (Rydall & Macdonald, 1992b). Note that these levels are far below those required to induce the appearance of nonbilayer phases as detected using ^{31}P NMR (Rydall & Macdonald, 1992b).

The ^2H NMR spectra clearly indicate that δ-toxin perturbs only one side of the lipid bilayer when added asymmetrically. It follows that δ-toxin does not span the lipid bilayer since such a transmembrane orientation should perturb both monolayers of the bilayer to some degree. Consequently, a surface orientation for δ-toxin is strongly indicated.

Further support for this conclusion is provided by a quantitative analysis of the quadrupole splittings measured before and after freeze-thawing of the GUVs exposed to δ-toxin. Prior to freeze–thawing, the value of the quadrupole splitting from the lipid population exposed to δ-toxin (5.00 kHz) corresponds to an effective peptide-to-lipid ratio of 1/13 (Rydall and Macdonald, 1992b), or about twice the overall ratio initially added. After freeze–thawing (spectrum c) a single Pake pattern is obtained, and the value of its quadrupole splitting (5.51 kHz) corresponds to an effective peptide-to-lipid ratio of 1/25, precisely the ratio added initially. Since δ-toxin binding to lipid membranes is virtually quantitative at such levels, there is only one possible interpretation of these observations. Upon addition of δ-toxin to the external vesicle solution, it binds to and remains localized at the bilayer surface. The effective peptide-to-lipid ratio is twice the overall sample ratio because half the lipids are sequestered from exposure to δ-toxin binding. After freeze–thawing of the GUVs and complete equilibration of the internal and external vesicle solutions, the δ-toxin redistributes symmetrically between the inner and outer monolayers of the bilayer. Since the entire lipid population is now exposed to peptide binding, the effective peptide-to-lipid ratio corresponds to the global ratio.

It is interesting that for the case of δ-toxin binding it is not possible to reproduce the "two-population" spectrum (b) simply by a 1:1 addition of the two end-point "one-population" spectra (a + c). This reflects the very different equilibrium binding association constants for δ-toxin versus perchlorate or calcium ions. Because δ-toxin binds with such high affinity, levels of binding approach 100%. Freeze–thawing the GUVs and exposing both monolayers of the bilayer to peptide binding effectively doubles the exposed lipid bilayer surface area and produces a 2-fold decrease in the concentration of δ-toxin per unit of exposed membrane surface. Consequently, the peptide-exposed lipid populations before and after freeze–thawing differ significantly in terms of their effective peptide-to-lipid ratios, and a 1:1 addition of the two "one-population" spectra must not reproduce the "two-population" spectrum. In contrast, perchlorate or calcium ions bind with relatively low affinity and the free ligand concentrations are sufficient to approach saturation binding levels both before and after freeze–thawing. Consequently, the ion-exposed populations before and after freeze–thawing do not differ significantly, and the 1:1 spectral addition procedure is valid.

CONCLUDING REMARKS

The results presented here are the first demonstration of the use of ^2H NMR to resolve differences in lipid head group conformation and orientational order at the inner versus outer monolayer in unilamellar lipid bilayer vesicles. Changes in conformation may be induced by means of the well-known response of phosphatidylcholine to membrane surface charge. Changes in head group orientational order may be induced by the addition of either peptides or other biological compounds to the membrane. This new capability offers an additional dimension to membrane research and paves the way for investigations of a new range of phenomena related to transmembrane asymmetry previously inaccessible to ^2H NMR.

Some issues which may now be amenable to ^2H NMR investigation include (1) the topography of protein insertion

into membranes, (2) transmembrane electrical potential-dependent protein conformation, (3) asymmetry of transmembrane lipid distribution, (4) equilibrium distribution of bioactive molecules, (5) the mechanism of vesicle fusion, and (6) those mechanical properties of membranes which influence lipid order, such as bilayer undulations.

Many proteins insert asymmetrically into membranes and, once inserted, retain the preferred orientation owing to a negligible rate of protein flip-flop. Such proteins often contain terminal amino acid residues of different charges; therefore, in the event of asymmetric transmembrane insertion, the protein will elicit a separate ^{2}H NMR signal from phosphatidylcholine located in the inner versus outer leaflets of the membrane. Furthermore, it will be possible to distinguish the case where protein insertion is not membrane-spanning but only partial, or where the protein does not insert but associates only superficially with the membrane. For electrically neutral membrane proteins, or proteins such as δ-toxin that are charged but do not elicit a charge response from the choline head group, their influence on lipid orientational order provides a means to address similar issues. Additionally, owing to the capability of imposing an electrical transmembrane potential in GUVs, it becomes feasible to investigate the role of the latter in determining the topography of protein insertion as well as the conformation of those proteins, such as alamethicin, that are affected by transmembrane electrical potentials.

Cullis and co-workers have shown that it is possible to induce lipid asymmetry in response to a transmembrane pH gradient in membranes containing either phosphatidic acid or phosphatidylglycerol (Hope et al., 1992). However, this phenomenon is not so readily quantified, and it is in this respect that ^{2}H NMR measurements may provide a direct, quantitative evaluation of the equilibrium distribution of such charged phospholipids on both sides of the bilayer simultaneously. Likewise, the equilibrium transmembrane distribution of such compounds as anesthetics, electrical potential sensitive dyes, and certain drugs may be determined, provided that these compounds are charged and that they elicit a ^{2}H NMR-detectable conformational response in the head group of phosphatidylcholine.

The nature of membrane surface undulations and their effect on lipid order are an important issue in the field of membrane material properties [for a review see Bloom and Evans (1992)]. In unilamellar vesicles transmembrane osmotic gradients can be imposed that modulate the amplitude of membrane undulations. In theory these should influence lipid ^{2}H NMR parameters such as the T_2 relaxation time and orientational order parameter, but experimental confirmation is still lacking. The combination of ^{2}H NMR and GUVs renders such phenomena accessible to investigation.

REFERENCES

Akutsu, H., & Seelig, J. (1981) *Biochemistry 20*, 7366–7373.
Aloy, M. M., & Rabaut, C. (1913) *Bull. Soc. Chim. Fr. 13*, 457–460.
Altenbach, C., & Seelig, J. (1984) *Biochemistry 23*, 3913–3920.
Altenbach, C., & Seelig, J. (1985) *Biochim. Biophys. Acta 818*, 410–415.
Aneja, R., Chada, J. S., & Davies, A. P. (1970) *Biochim. Biophys. Acta 218*, 102–111.
Bayerl, T. M., & Bloom, M. (1990) *Biophys. J. 58*, 357–362.
Berne, B. J., & Pecora, R. (1976) *Dynamic Light Scattering with Applications to Chemistry, Biology and Physics*, Wiley, New York.
Beschiaschvili, G. & Seelig, J. (1991) *Biochim. Biophys. Acta 1061*, 78–84.
Bloom, M., & Evans, E. (1992) *Biologically Inspired Physics, Nato ASI Ser., Ser. B 263*, 137-147.
Bloom, M., Burnell, E. E., Valic, M. I., & Weeks, G. (1975) *Chem. Phys. Lipids 14*, 107–112.
Brown, M. F., & Seelig, J. (1978) *Biochemistry 17*, 381–384.
Browning, J. (1981) *Biochemistry 20*, 7144–7151.
Burnell, E. E., Cullis, P. R., & De Kruijff, B. (1980) *Biochim. Biophys. Acta 603*, 63–69.
Comfurius, P., & Zwaal, R. F. A. (1977) *Biochim. Biophys. Acta 488*, 36–42.
Davis, J. H. (1983) *Biochim. Biophys. Acta 737*, 117–171.
Davis, J. H., Jeffrey, K. R., Bloom, M., Valic, M. I., & Higgs, T. P. (1976) *Chem. Phys. Lett. 42*, 390–394.
Edidin, M. (1981) in *Membrane Structure* (Finean, J. B., & Michell, R. H., Eds.) pp. 37–82, Elsevier, New York.
Evans, E., & Needham, D. (1987) *J. Chem. Phys. 91*, 4219–4228.
Freer, J. H., & Arbuthnott, J. P. (1982) *Pharmacol. Ther. 19*, 55–106.
Freer, J. H., & Birkbeck, T. H. (1982) *J. Theor. Biol. 94*, 535–540.
Gale, P., & Watts, A. (1992) *Biochim. Biophys. Acta 1106*, 317–324.
Gent, M. P. N, & Prestegard, J. H. (1974) *Biochemistry 13*, 4027–4033
Goldin, S. M. (1977) *J. Biol. Chem. 252*, 5630–5642.
Griffin, R. G. (1981) *Methods Enzymol. 72*, 108–174.
Harbisson, G. S., & Griffin, R. G. (1984) *J. Lipid Res. 25*, 1140–1142.
Hope, M. J., Bally, M. B., Webb, G., & Cullis, P. R. (1985) *Biochim. Biophys. Acta 812*, 55–65.
Hope, M. J., Redelmeier, T. E., Wong, K. F., Rodrigueza, W., & Cullis, P. R. (1989) *Biochemistry 28*, 4181–4187.
Lasic, D. D. (1982) *Biochim. Biophys. Acta 692*, 501–502.
Macdonald, P. M., & Seelig, J. (1987a) *Biochemistry 26*, 1231–1240.
Macdonald, P. M., & Seelig, J. (1987b) *Biochemistry 26*, 6292–6298.
Macdonald, P. M. ,& Seelig, J. (1988) *Biochemistry 27*, 6769–6775.
Macdonald, P. M., Leisen, J., & Marassi, F. M. (1991) *Biochemistry 30*, 3558–3566.
Philippot, J., Mutaftschiev, S, & Liautard, J. P. (1983) *Biochim. Biophys. Acta 734*, 137–143.
Pike, E. R. (1981) in *Scattering Techniques Applied to Supramolecular and Nonequilibrium Systems* (Chen, S. H., Chu, B., & Nossal, R., Eds.) Plenum Press, New York.
Rance, M., & Byrd, R. A. (1983) *J. Magn. Reson. 52*, 221–240.
Rhoden, V., & Goldin, S. M. (1979) *Biochemistry 18*, 4173–4176.
Ryba, N. J. P., Dempsey, C. E., & Watts, A. (1986) *Biochemistry 25*, 4818–4825.
Rydall, J. R., & Macdonald, P. M. (1992a) *Biochemistry 31*, 1092–1099.
Rydall, J. R., & Macdonald, P. M. (1992b) *Biochim. Biophys. Acta 1111*, 211–220.
Saunders, L, Perrin, J., & Gammack, D. B. (1962) *J. Pharm. Pharmacol. 14*, 567-572.
Scherer, P. G. & Seelig, J. (1989) *Biochemistry 28*, 7720–7728.
Seelig, J. (1977) *Q. Rev. Biophys. 10*, 353–418.
Seelig, J., Macdonald, P. M., & Scherer, P. G. (1987) *Biochemistry 26*, 7535–7541.
Shivers, R. R., & Brightman, M. W. (1976) *J. Comp. Neurol. 167*, 1–8.
Skarjune, R., & Oldfield, E. (1979) *Biochemistry 18*, 5903–5909.
Sternin, E., Bloom, M., & MacKay, A. L. (1983) *J. Magn. Reson. 55*, 274–282.
Stockton, W. G., Polnaszek, C. F., Tulloch, A. P., Hasan, F., & Smith, I. C. P. (1976) *Biochemistry 15*, 954–966.
Terwilliger, T. C., Weissman, L., & Eisenberg, D. (1982) *Biophys. J. 37*, 353–361.